JOURNAL OF SPACECRAFT AND ROCKETS
Vol. 39, No. 5, September–October 2002

Rationale for Defining Structural Requirements for Large Space Telescopes

Mark S. Lake*
Composite Technology Development, Inc., Lafayette, Colorado 80026
Lee D. Peterson†
University of Colorado, Boulder, Colorado 80309
and
Marie B. Levine‡
Jet Propulsion Laboratory, California Institute of Technology, Pasadena, California 91109

A rationale is presented for defining structural requirements for future large space telescope systems. The rationale is based on bounding linear analyses for the deformation of telescope mirrors in response to expected on-orbit disturbance loads and consideration of active control systems that partially compensate for these deformations. It is shown that the vibration frequency of the telescope structure, independent of telescope size, determines the passive structural stability and requirements for an active control system. This means that future large telescopes with low vibration frequencies will necessarily allocate increased active control error budget in proportion to the square of the vibration frequency. Parametric analyses are also presented for the vibration response of two representative mirror architectures: a tensioned membrane mirror and a truss-supported segmented mirror. These examples demonstrate that meeting a specified frequency requirement will require a trade between structural mass fraction and depth of the primary mirror support structure regardless of the structural architecture.

Nomenclature

$\{A_I\}$	=	inertial acceleration vector, m/s^2 (in./s^2)
$\lvert A_I \rvert$	=	magnitude of inertial acceleration vector, m/s^2 (in./s^2)
a_n	=	nth mode participation factor for acceleration
a_{rms}	=	rms magnitude of acceleration vector, m/s^2 (in./s^2)
D_{plate}	=	equivalent bending stiffness of truss-supported segmented reflector, N · m (lbf · in.)
d	=	diameter of telescope mirror, m (ft)
$(EA)_{\text{torus}}$	=	circumferential stiffness of torus structure, N (lbf)
$(EAL)_{\text{truss}}$	=	average axial stiffness times length of truss member, N · m (lbf · in.)
$(EI)_{\text{torus}}$	=	flexural stiffness of torus structure, N · m^2 (lbf · in.^{2})
$(E/\rho)_{\text{torus}}$	=	specific modulus of torus structure, m^2/s^2 (in.^{2}/s^2)
$(E/\rho)_{\text{truss}}$	=	specific modulus of truss structure, m^2/s^2 (in.^{2}/s^2)
$\{F_I\}$	=	d'Alembert inertial force vector, N (lbf)
f_0	=	lowest frequency, Hz
h	=	depth of mirror support structure, m (ft)
$[K]$	=	stiffness matrix, N/m (lbf/in.)
k	=	solar reflectance coefficient
$[M]$	=	mass matrix, kg (lbm)
$M_{\text{reflector}}$	=	mass of reflector surface, kg (lbm)
$M_{\text{structure}}$	=	mass of reflector support structure, kg (lbm)
N_{panels}	=	number of reflector panels in truss-supported segmented reflector
N_{rings}	=	number of rings of reflector panels in truss-supported segmented reflector
N_{struts}	=	number of truss struts in truss-supported segmented reflector
p_{solar}	=	solar pressure, N/m^2 (lbf/in.^{2})
R	=	orbital radius, m (ft)
R_{solar}	=	distance from sun, astronomical units
T_{orb}	=	orbital period, s
T_{slew}	=	slew period, s
$\{X_I\}$	=	displacement response vector, m (in.)
$\{X_n\}$	=	nth eigenvector, that is, normal mode, m (in.)
x_n	=	nth mode participation factor for displacement
x_{rms}	=	rms magnitude of displacement vector, m (ft)
ζ	=	modal damping coefficient
η	=	structural mass fraction
κ	=	structural load factor
μ	=	gravitational attraction force, m^3/s^2 (in.^{3}/s^2)
$(\rho AL)_{\text{truss}}$	=	mass of truss member, kg (lbm)
ρ_{areal}	=	average areal density of reflector system, kg/m^2 (lbm/in.^{2})
ω_n	=	nth eigenvalue, s^{-1}
ω_0	=	lowest eigenvalue, s^{-1}

Introduction

THE past several decades have been a period of dramatic revolution in technologies and concepts for large telescopes for both ground and space applications. Two important enabling technologies that have evolved substantially are active alignment control of optical segments and adaptive correction of optical wave front errors. For ground-based telescope systems, these active control technologies have been applied mainly in efforts to correct for poor "seeing" conditions through the Earth's atmosphere. For space-based telescope applications, these active control technologies have the potential to make practical much larger and lighter weight telescope designs by reducing the requirements for passive stability in the telescope structure.

Traditionally, telescope designs have achieved the necessary passive stability through the use of thick optical segments made of stable (but low specific stiffness) materials and massive metering structures. In the future, and especially for space-based telescope applications, it is clear that more efficient materials and structural concepts will be used to reduce mass and that active control systems will be used to compensate for instabilities in the

Received 23 May 2001; revision received 8 February 2002; accepted for publication 28 May 2002.

*Chief Engineer, 1505 Coal Creek Drive. Associate Fellow AIAA.
†Associate Professor, Department of Aerospace Engineering Sciences, Campus Box 420. Associate Fellow AIAA.
‡Senior Research Engineer, Science and Technology Development Section, M/S 157-317. Member AIAA.

structure. An important question is then, what rationale should be applied in suballocating system stability requirements between the structure and the active control systems for future large space telescopes?

To answer this question it is necessary to have some insight into the design of both active control systems and structures. Specifically, it is necessary to appreciate the total "cost," that is, financial burden, development risk, system mass, etc., of exclusively active and exclusively passive designs. Also, it is necessary to understand the "cost breakpoints" on dimensional stability, that is, the dimensional stability above or below which either the passive or the active solutions become excessively costly.

This paper will discuss several issues that affect substantially the conceptual design of a telescope structure. These issues include the overall size and mass goals of future missions, the on-orbit disturbance load environment, and the efficiency of various structural concepts. One purpose of this paper is to provide a means for quantifying the cost of achieving a particular dimensional stability requirement passively through proper structural design. Implicitly, these analyses are intended to provide a reasonable and thoughtful basis for one to begin assessing quantitatively the cost breakpoints in passive structural design. Ultimately, it is hoped that these analyses will stimulate a movement toward the application of disciplined, analytically grounded (and less arbitrary) rationale for the suballocation of overall dimensional stability requirements between the structure and the active control systems.

It is hoped that the present paper will provoke the development of similar analyses to characterize the cost and cost breakpoint of active control solutions so that, ultimately, future system engineers will have a more complete set of tools with which to perform thoughtful system trade studies. By itself, the present paper is intended to provide a basis for the definition of top-level structural requirements that are derived from the first principles of structural design and that are at least consistent with a broad understanding of the capability and cost of active control systems.

Future Trends in Astronomical Space Telescopes

The future science goals of the ultraviolet–optical–infrared (UVOIR) astronomy community include detailed study of the birth and evolution of distant galaxies and planetary systems.[1] The principal space-based observatory under development to make these measurements is the Next Generation Space Telescope (NGST).[2] The 8-m-diam aperture of the NGST will be capable of imaging fainter objects in shorter integration times and, hence, will deliver more science through-put than the current Hubble Space Telescope (HST). However, with 10 times the collecting area and approximately the same mass as the HST primary mirror, the NGST primary mirror will have much lower vibration frequencies and be much more sensitive to on-orbit loading than the HST mirror. Two factors that distinguish the NGST mirror from the HST mirror, and that allow the NGST mirror to be so much larger and lighter weight, are the use of active alignment control and the selection of an orbit that is a very benign loading environment.

Beyond NGST, the UVOIR astronomy community is envisioning even larger filled-aperture space telescopes and interferometers. Specifically, 20-m-class filled-aperture space telescopes are envisioned after 2010. Recent studies of 20-m-class space telescopes have focused on "gossamer" telescopes, which are extremely lightweight, having areal densities possibly on the order of 1 kg/m^2. Such telescopes would use thin membrane optics coupled with active wave front control. Most likely, these mirrors will have less stiffness, that is, lower frequencies, than the NGST mirror and will be much more sensitive to disturbance loads.

Traditionally, ground-based telescope systems have been designed to exhibit vibration frequencies on the order of hundreds of hertz. Experience has shown that systems with frequencies this high tend to exhibit sufficiently small elastic response such that they maintain alignment while being slewed in the presence of Earth's gravity. Of course, the inertial loads for space-based telescopes are substantially lower than the inertial loads for ground-based telescopes. This benign loading environment, coupled with the expected use of active control systems on future space telescopes, demands thoughtful reconsideration of vibration frequency requirements. Specifically, it is clear that future space-based telescope optics will not be required to exhibit fundamental frequencies as high as several hundred hertz (as was the case for HST). In fact, reducing vibration frequency requirements is necessary to achieve the large size and low masses projected for future space-based telescopes. The next section develops the analytical basis for establishing structural requirements for future space-based telescopes.

Disturbance Loads and Structural vs Active Control Requirements

The disturbance loads that can affect the dimensional precision of a large space telescope include thermal loads, inertial loads (e.g., slew loads, gravity gradient loads, and solar-pressure loads), and loads from onboard machinery, for example, control moment gyros and cryocoolers. Thermal loads are not considered in the present study, but are of critical importance in the selection of materials and the use of thermal control systems.

In general, inertial loads are slowly varying in time, and optical distortions due to these loads can be estimated by static-response analysis. Disturbance loads from onboard machinery are typically broadband in frequency content and can lead to structural resonances if the disturbances are not attenuated to acceptable levels through active or passive isolation systems. It will be shown that linear analyses can provide reasonable upper bounds for the optical distortions to both inertial and onboard disturbance loads.

Effect of Frequency on Response to Quasi-Static Inertial Loads

An upper bound on the rms deformation in a telescope mirror due to a quasi-static inertial load is derived in Appendix A and given by

$$x_{\text{rms}} \leq \frac{a_{\text{rms}}}{4\pi^2 f_0^2} \tag{1}$$

where f_0 is the fundamental natural frequency of the telescope mirror (in hertz) and a_{rms} is the rms magnitude of the acceleration associated with the disturbance load. Note that Eq. (1) does not include any structural dimensions. This result implies that two different sized telescopes with equal vibration frequencies can be expected to have similar response magnitudes for the same inertial disturbances.

Figure 1 presents a plot of Eq. (1) for four values of the fundamental natural frequency f_0 (ranging from 0.1 to 100 Hz). The abscissa represents the inertial disturbance magnitude a_{rms} (in gravitational acceleration units) and the ordinate represents the elastic deformation magnitude x_{rms}. Overlaid within Fig. 1 are approximate disturbance-rejection bands for both ground and space telescopes. These bands indicate the rough order of magnitude upper and lower bounds on disturbance accelerations and response magnitudes that must be accommodated for by the telescope structure and/or active alignment control system. (See Appendix B for order of magnitude analysis of inertial disturbance loads for space telescopes.)

Figure 1 provides a means for estimating rough order of magnitude active control system requirements. Given a value of structural response frequency, the line associated with that frequency provides an upper bound on the elastic response of the structure across the

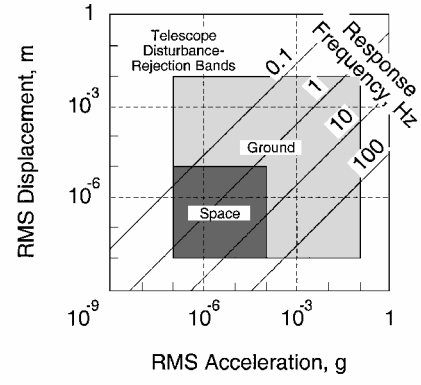

Fig. 1 Relationship between displacement, acceleration, and frequency for quasi-static loading.

spectrum of quasi-static disturbance loads. Therefore, the portion of the disturbance-rejection band above the response frequency line is accommodated passively by the inherent stiffness of the structure. On the other hand, the portion of the disturbance-rejection band below the response frequency line must be accommodated by the active control system.

Ground telescopes typically exhibit vibration frequencies on the order of hundreds of hertz. Figure 1 indicates that ground telescope systems with frequencies this high can be expected to accommodate most inertial disturbances passively. Similarly, the HST exhibits fundamental frequencies well above 100 Hz, and Fig. 1 indicates that this frequency is high enough to accommodate essentially all on-orbit disturbances passively. On the other hand, the primary mirror of the NGST is expected to exhibit a fundamental frequency on the order of 10 Hz. This frequency is high enough to accommodate most expected disturbances passively. To accommodate all possible disturbances, the NGST mirror will also incorporate quasi-static realignment capability in its primary mirror.

Another important observation about future gossamer architectures can also be made from Fig. 1. The sensitivity of the structure to disturbances increases with the square of the decrease in structural frequency. Figure 1 indicates that a 0.1-Hz gossamer telescope can tolerate only nano gravitational acceleration unit disturbances passively; thus, such a telescope will be a nearly completely active system. In fact, a telescope with a 0.1-Hz frequency would require an active control system with 10,000 times more authority than is planned for NGST. Clearly, in this case, the cost of increased structural mass for higher frequency must be balanced against the cost and risk associated with a 10,000-fold increase in control capability.

Furthermore, the analyses in Appendix B suggest that, although it is possible to reduce inertial loads by prudent selection of orbit and operational considerations, for example, slew-rate limitations, it is also prudent to assume some lower limit of uncertainty for inertial loading that must be tolerated by the mirror. For example, it might be reasonable to assume that any mirror system must tolerate at least 1 μg of uncertainty in inertial loading during operations. From Fig. 1, a 1-μg inertial disturbance results in a few nanometers of deformation in a 10-Hz system and a few hundred nanometers of deformation in a 1-Hz system. Clearly, a 1-μg uncertainty in inertial loading is of little consequence to a mirror with a 10-Hz first frequency, but it could be significant to a mirror with a 1-Hz first frequency. Similarly, a 0.1-Hz mirror would experience many micrometers of deformation. This illustrates the importance of maintaining a reasonably high-frequency requirement even for gossamer membrane mirrors.

Effect of Damping on Response to Broadband Loads

As mentioned earlier, the main sources of dynamic loads for a space telescope are onboard machinery such as cryocoolers and reaction-control wheels. Typically, the disturbance spectra from these devices will be attenuated to acceptable levels through active or passive isolation systems. However, some residual dynamic disturbance is to be expected.

Next to fundamental frequency, the most important parameter for determining the response of a telescope structure to dynamic loading is damping. In general, the dynamic response to a broadband load will depend on the modal complexity and the specific power spectral density of the load. However, it is possible to gain design insight by considering the special case of a nearly harmonic load because many dynamic disturbances onboard spacecraft are harmonic. In this case, the upper bound on response to dynamic loading is

$$x_{\text{rms}} \leq \left(\frac{1}{2\zeta}\right)\frac{a_{\text{rms}}}{4\pi^2 f_0^2} \tag{2}$$

A typical value for damping in mechanically jointed telescope structures is $\zeta \approx 0.01$ (or 1%), which leads to a magnification factor ($1/2\zeta$ of 50. It is hard to estimate the damping to be expected in a membrane gossamer telescope, but it is reasonable to assume that damping could be somewhat higher than in mechanically jointed telescope assemblies, for example, $\zeta \approx 0.01$–0.05 (or 1–5%) might be typical. In either case, membrane or mechanically jointed telescopes, dynamic disturbances that encompass the fundamental frequency of the structure can cause deformations one to two orders of magnitude larger than deformations from quasi-static loading.

In general, passive damping in an optical system is a double-edged sword. Damping is desirable to mitigate distortions due to broadband disturbances. However, in state-of-the-art precision deployable structures (including NGST), damping is intentionally kept to a minimum to minimize microdynamic dimensional instability.[3] In addition, many future space telescopes are being designed to operate at cryogenic temperatures where passive material damping is expected to be substantially lower than 1%. Therefore, although one might prefer to have high passive damping to mitigate broadband disturbances, it is likely that passive damping will be low in future space telescope systems. This result indicates the importance of attenuating broadband dynamic disturbances through isolation or augmented damping of the telescope structure. This result also indicates the importance of designing the fundamental frequency of the telescope assembly as high as possible.

Trade Between Structural Depth and Mass Fraction

This section is intended to convey some insight into the problem of designing a large optical reflector to meet a specified frequency requirement. Two mirror architectures are considered: a truss-supported segmented reflector and a tensioned membrane reflector. Through approximate analyses, explicit analytical expressions are derived for the fundamental frequencies of both reflectors. These expressions are written in terms of three key design parameters for the reflector support structure: structural mass fraction, depth-to-diameter ratio, and material specific stiffness. Finally, these expressions are used to illustrate the trade that can be made between mass fraction and depth to achieve a specified vibration frequency.

Truss-Supported Segmented Reflector

A truss-supported segmented reflector is shown in Fig. 2. Analyses of the free–free vibration of reflectors of various sizes are presented in Ref. 4. In these analyses, the reflector panels, mechanical joints, and any other nonstructural components are treated as parasitic mass, and the stiffness is determined from the truss only. The fundamental vibration mode was found to be an anticlastic bending, that is, "saddle," mode of the reflector system.

From the results in Ref. 4, it can be shown that the fundamental free–free vibration frequency (in hertz) of a truss-supported segmented reflector with small depth-to-diameter ratios, that is, $h/d < 0.2$, can be approximated by

$$(f_0)_{\text{segmented}} = \frac{3.343}{d^2}\sqrt{\frac{D_{\text{plate}}}{\rho_{\text{areal}}}} \tag{3}$$

where D_{plate} and ρ_{areal} are the equivalent bending stiffness and areal density of the reflector given, respectively, by

$$D_{\text{plate}} = \frac{\sqrt{3}(EAL)_{\text{truss}}}{4}$$

$$\rho_{\text{areal}} = \frac{1}{\eta}\left[\frac{N_{\text{struts}}(\rho AL)_{\text{truss}}}{3\sqrt{3}d^2/8}\right] \tag{4}$$

The parameters $(EAL)_{\text{truss}}$ and $(\rho AL)_{\text{truss}}$ in Eq. (4) are the average axial stiffness (times length) and mass, respectively, of each strut in

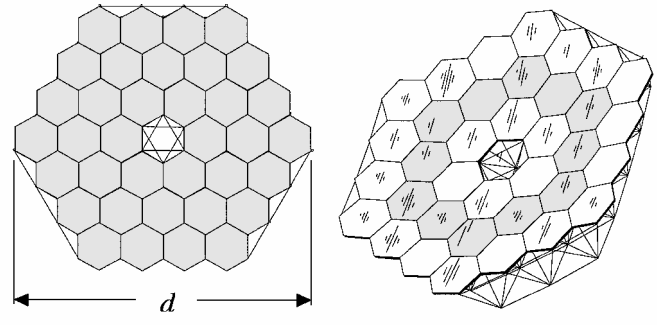

Fig. 2 Truss-supported segmented reflector.

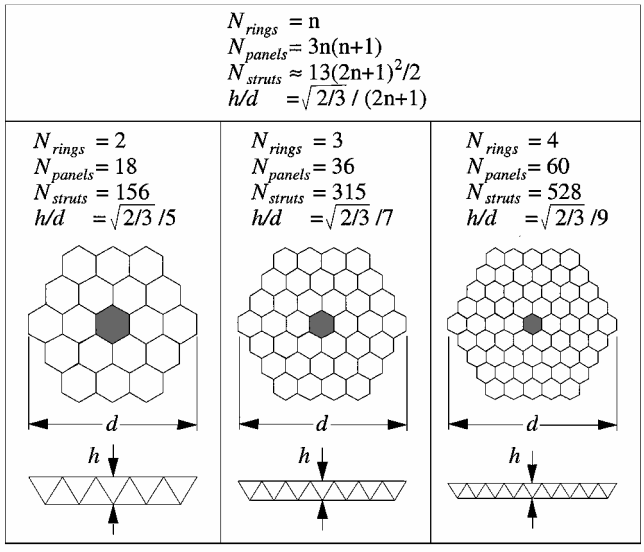

Fig. 3 Part counts and diameter-to-depth ratios for truss-supported segmented reflectors.

the support truss. N_{strut} is the number of struts in the support truss, and η is defined as

$$\eta \equiv \frac{\text{truss mass}}{\text{total mass}} \tag{5}$$

Substituting Eqs. (4) into Eq. (3) and simplifying gives

$$(f_0)_{\text{segmented}} = (1.773/d)\sqrt{(\eta/N_{\text{struts}})(E/\rho)_{\text{truss}}} \tag{6}$$

Figure 3 presents three truss-supported segmented reflectors with two to four rings of reflector panels, respectively. Also included in Fig. 3 are the number of reflector panels and truss struts associated with each reflector geometry and general expressions for these part counts as functions of the number of rings of panels, N_{rings}. Finally, Fig. 3 includes a general expression for the truss depth ratio h/d as a function of N_{rings}. From these expressions, it can be shown that

$$N_{\text{struts}} \approx \frac{13}{3(h/d)^2} \tag{7}$$

Substituting Eq. (7) into Eq. (6) gives

$$(f_0)_{\text{segmented}} = (0.852/d)(h/d)\sqrt{\eta(E/\rho)_{\text{truss}}} \tag{8}$$

Equation (8) is an approximate expression for the fundamental free–free vibration frequency (in hertz) of a truss-supported segmented reflector. The frequency is proportional to the depth-to-diameter ratio h/d, the square root of the structural mass fraction η, and the specific modulus E/ρ of the truss. Also, the frequency is inversely proportional to the diameter d. Figure 4 plots this frequency for two diameters, 10 and 100 m and ranges of η and h/d. In Fig. 4, it is assumed that the support truss is made of a composite material with $E = 104$ GPa (15×10^6 psi) and $\rho = 0.0017$ kg/cm^3 (0.06 lbm/in.^{3}), hence $(E/\rho)_{\text{truss}} = 61.2 \times 10^6$ m^2/s^2 (9.5×10^{10} in.^{2}/s^2).

The upper grid of data points in Fig. 4 is associated with a reflector diameter of 10 m and the lower grid of data points is associated with a reflector diameter of 100 m. The grids are identical and separated by one order of magnitude in frequency. A log scale is provided on the right for interpolating to other values of diameter. Figure 4 (or a similar plot for another value of E/ρ) provides a convenient means for quickly assessing the trade between truss depth ratio and mass fraction for a given frequency requirement and a given reflector diameter.

Tensioned Membrane Reflector

This section presents analysis of the fundamental vibration frequency of a flat circular membrane reflector that is tensioned by a toroidal compression structure (Fig. 5). These analyses should indicate the performance to be expected out of other tensioned membrane reflector designs, for example, singly curved and doubly

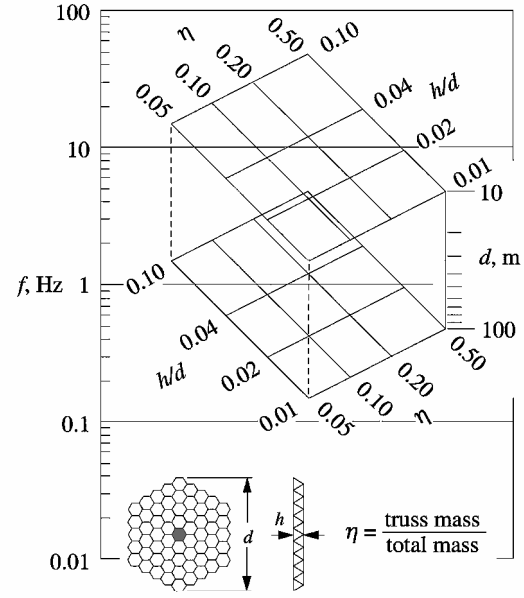

Fig. 4 Approximate frequency of truss-supported segmented reflector: $(E/\rho)_{\text{truss}} = 61.2 \times 10^6$ m^2/s^2.

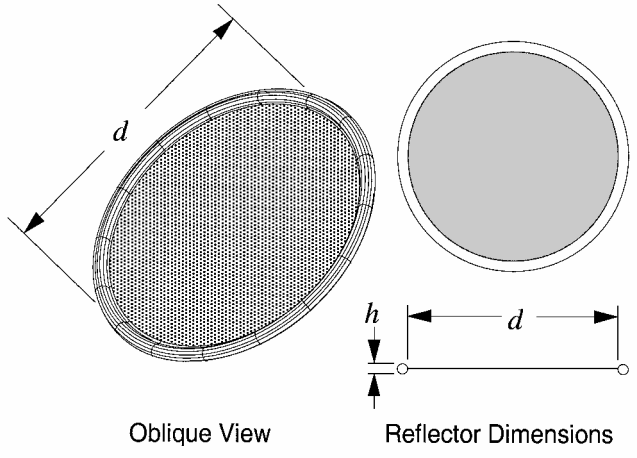

Fig. 5 Circular membrane reflector tensioned by a perimeter toroidal structure.

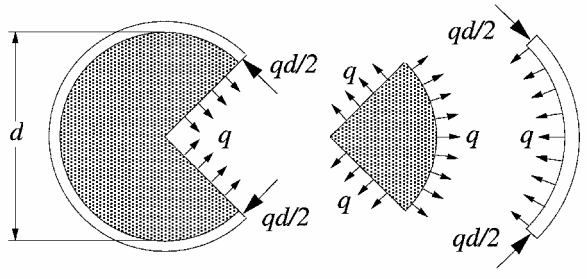

Fig. 6 Load distribution within a circular membrane and a toroidal tensioning structure.

curved membranes. The key design consideration included in these analyses is that the perimeter structure must be sized with sufficient strength, that is, depth, to react the tension load that it applies to the membrane.

A fundamental vibration mode of a membrane tensioned by a perimeter structure can be either a pure membrane mode or a coupled membrane and perimeter structure mode. For simplicity, the vibration mode considered herein is the fundamental mode of the membrane. It is assumed that the perimeter structure provides sufficient stiffness such that the edge of the membrane is motionless and that the stress field throughout the membrane is constant and uniform. Figure 6 presents the loading condition that exists between the membrane and the perimeter structure.

Blevins[5] showed that the fundamental lateral frequency of a circular tensioned membrane that is pinned along its boundary is (in hertz)

$$(f_0)_{\text{membrane}} = 0.678\sqrt{q/M_{\text{membrane}}} \tag{9}$$

where q is the uniform stress resultant associated with the membrane tension, that is, in-plane stress times thickness, and M_{membrane} is the mass of the membrane.

The perimeter structure must have adequate depth and stiffness to resist lateral buckling in reaction to the membrane tension q (Fig. 6). The critical stress resultant q_{cr}, for a circular toroidal beam is[6]

$$q_{\text{cr}} = \left[24(EI)_{\text{torus}}/d^3\right]\{1/[1 + (EI/4GJ)_{\text{torus}}]\} \tag{10}$$

where EI and GJ are the flexural and torsional stiffnesses of the torus. If the torus cross section is circular, $J = 2I$, and if the torus material is isotropic, $G = E/[2(1+\nu)] \approx 3E/8$. Thus, Eq. (10) simplifies to

$$q_{\text{cr}} = 18(EI)_{\text{torus}}/d^3 \tag{11}$$

It is possible to relate the critical buckling stress of the torus q_{cr} to the membrane tension q by introducing the structural load factor $\kappa \equiv q/q_{\text{cr}}$, or

$$q = \kappa q_{\text{cr}} = 18\kappa(EI)_{\text{torus}}/d^3 \tag{12}$$

Substituting Eq. (12) into Eq. (9) and simplifying gives

$$(f_0)_{\text{membrane}} = 0.678\sqrt{\frac{18\kappa(EI)_{\text{torus}}}{d^3 M_{\text{membrane}}}} \tag{13}$$

If the torus has a thin circular cross section with a diameter h, the flexural stiffness of the torus $(EI)_{\text{torus}}$ can be written as

$$(EI)_{\text{torus}} = (h^2/8)(EA)_{\text{torus}} \tag{14}$$

where $(EA)_{\text{torus}}$ is the extensional stiffness of the cross section. Substituting Eq. (14) into Eq. (13) gives

$$\begin{aligned}(f_0)_{\text{membrane}} &= 0.678\sqrt{\frac{9\kappa h^2(EA)_{\text{torus}}}{4d^3 M_{\text{membrane}}}} \\ &= 0.678\sqrt{\frac{9\kappa h^2 E_{\text{torus}}[(\rho A)_{\text{torus}}\pi d]}{4\pi d^4 \rho_{\text{torus}} M_{\text{membrane}}}} \\ &= \frac{0.574}{d}\left(\frac{h}{d}\right)\sqrt{\kappa\left(\frac{E}{\rho}\right)_{\text{torus}}\frac{M_{\text{torus}}}{M_{\text{membrane}}}}\end{aligned} \tag{15}$$

Similar to Eq. (5) for the structural mass fraction of the segmented reflector, a structural mass fraction can be defined for the membrane reflector as

$$\eta \equiv \frac{M_{\text{torus}}}{M_{\text{torus}} + M_{\text{membrane}}} \tag{16}$$

Rearranging Eq. (16) and substituting the result into Eq. (15) gives the following fundamental frequency:

$$(f_0)_{\text{membrane}} = \frac{0.574}{d}\left(\frac{h}{d}\right)\sqrt{\frac{\kappa\eta(E/\rho)_{\text{torus}}}{(1-\eta)}} \tag{17}$$

Figure 7 presents a plot of Eq. (17) for ranges of the diameter, mass fraction, and depth ratio. In Fig. 7, it is assumed that the membrane tension load is one-half the load required to buckle the torus, that is, $\kappa = \frac{1}{2}$, and the torus is made of an isotropic material with $(E/\rho)_{\text{torus}} = 61.2 \times 10^6$ m^2/s^2 (9.5×10^{10} in.^{2}/s^2).

Compare the equations for fundamental vibration frequency of the truss-supported segmented reflector [Eq. (8)] and the tensioned membrane reflector [Eq. (17)]. Both frequencies are inversely proportional to the diameter of the reflector d, proportional to the depth ratio of the support structure h/d, and proportional to the square root of the specific modulus of the support structure E/ρ. In addition, for small structural mass fractions, for example, $\eta > 0.2$, both frequencies are approximately proportional to the square root of the mass fraction. The main difference between Eqs. (8) and (17) is the numerical constant and the presence of the structural load factor κ in Eq. (17).

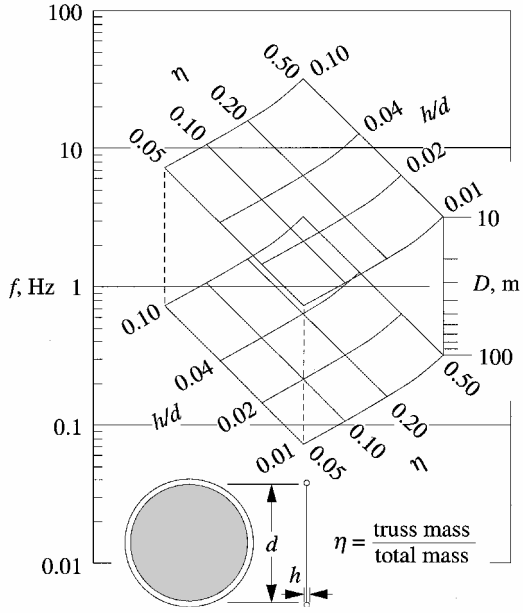

Fig. 7 Approximate frequency of tensioned membrane reflector: $\kappa = \frac{1}{2}$ and $(E/\rho)_{\text{torus}} = 61.2 \times 10^6$ m^2/s^2.

This comparison allows one to draw some general conclusions about the design of large-reflector structures. First, the similar form of Eqs. (8) and (17) suggests that other mirror architectures might exhibit similar vibration frequency relationships. Second, the key structural design parameters that affect the vibration frequency are structural mass fraction η and depth-to-diameter ratio h/d. Specifically, for a given frequency requirement, an increase in structural depth allows a decrease in structural mass and vice versa. Ultimately, the designers of future space telescopes must find an appropriate balance between structural depth and structural mass to satisfy a vibration frequency requirement.

Rationale for Defining Structural Requirements

As stated by Hedgepeth,[7] "the rational design of all structures must start with a definition of the task or function of the structure." Stated another way, without a clear definition of requirements for the structure, it is impossible to develop a design for the structure that can be verified.

It has been shown that fundamental frequency and damping are the most significant performance metrics for determining passive stability of a telescope structure. It has also been shown that structural mass fraction and depth ratio are key structural design parameters for determining vibration frequency. Therefore, it is critically important to include vibration frequency and damping among the top-level structural design requirements, and meeting these requirements will require a design trade between structural mass fraction and depth ratio.

To establish requirements on vibration frequency and damping, one must first consider the maximum figure error tolerated by the telescope system and the spectrum of disturbance loads expected during and between observations. Furthermore, one must consider the temporal and spatial bandwidth limitations of active control systems and possible nonlinear interactions between the control systems and the structure. Finally, one must consider the effects of uncertainties in all aspects of the design and must arrive at reasonable factors of safety to accommodate for these uncertainties. For example, it was shown that by assuming a lower limit of uncertainty in inertial loading during operations, for example, 1 μg, it is possible to establish a minimum frequency requirement that accommodates for this uncertainty passively, for example, 10 Hz.

Ultimately, a well-developed set of frequency and damping requirements should derive from consideration of the cost and performance of the structure and active control system options. Clearly, the historical approach of demanding optical-wavelength precision and stability in the structure is unnecessary and likely to lead back to designs that are massive and impractical. On the other hand, placing no demands on the structure by demanding that the active control systems accommodate all disturbances can easily lead to designs that are overly complex and risky. Common sense suggests that the most efficient, practical, and cost-effective telescope designs will include structural designs that achieve maximum practical passive stability through proper design and efficient use of the limited mass and depth allocations.

Conclusions

It has been shown that the vibration frequency and damping of the telescope structure, independent of telescope size, determines the passive structural stability and requirements for an active control system. Analyses of two representative mirror architectures, a tensioned membrane mirror and a truss-supported segmented mirror, have demonstrated that meeting a specified frequency requirement will require a trade between structural mass fraction and depth of the primary mirror support structure, regardless of the structural architecture. In other words, it has been shown that the cost of achieving a particular level of passive structural stability in a telescope mirror can be measured in terms of its structural mass and depth.

In general, future low-cost, that is, lightweight and thin, large telescopes with low vibration frequencies will necessarily allocate increased active control error budget in proportion to the square of the vibration frequency. Although this increased sensitivity to the disturbance environment could be partially offset by increased passive damping, it is likely that passive damping will be low in future space telescope systems. This situation dictates the need to attenuate broadband dynamic disturbances through isolation or augmented damping of the telescope structure. This situation also dictates the need to design the fundamental frequency of the telescope assembly to be as high as practical, that is, within definable limits on structural mass and depth.

From these analyses, a rationale has been presented for defining structural requirements for future large space telescope systems. The rationale is based on the derivation of an achievable and reasonable set of frequency and damping requirements considering the cost and performance of the structure and active control system options. The historical approach of demanding optical-wavelength precision and stability in the structure is impractical for future large space telescopes, whereas placing no demands on the structure by demanding that the active control systems accommodate all disturbances can easily lead to designs that are overly complex and risky. Common sense suggests that the most efficient, practical, and cost-effective telescope designs will include structural designs that achieve maximum practical passive stability through proper design and efficient use of the limited mass and depth allocations.

Appendix A: Deformation of a Space Telescope Under Quasi-Static Inertial Loading

The problem of determining the rms deformation in a telescope mirror due to a quasi-static inertial load can be solved generally by application of a modal expansion technique.[8] The mirror can be represented as an n-degree-of-freedom elastic system characterized by a mass matrix $[M]$ and stiffness matrix $[K]$. For this system, there exists an orthonormal set of eigenvectors $\{X_n\}$, that is, mode shapes, that satisfy

$$\left(1/\omega_n^2\right)\{X_n\} = [K]^{-1}[M]\{X_n\} \tag{A1a}$$

$$\{X_m\}^T\{X_n\} = \delta_{mn} \tag{A1b}$$

where ω_n are the eigenvalues, that is, natural frequencies, associated with the eigenvectors $\{X_n\}$.

Consider an inertial loading of the system defined by the following vector of d'Alembert forces $\{F_I\}$:

$$\{F_I\} = [M]\{A_I\} \tag{A2}$$

Following the principle of d'Alembert (see Ref. 9), the deformations $\{X_I\}$ resulting from this load can be determined from the following equivalent static problem:

$$\{X_I\} = [K]^{-1}[M]\{A_I\} \tag{A3}$$

Without loss of generality, the inertial acceleration vector $\{A_I\}$ and the inertial deformation vector $\{X_I\}$ can be expressed in terms of the basis of normal modes $\{X_n\}$ as follows:

$$\{X_I\} = x_n\{X_n\} \tag{A4a}$$

$$\{A_I\} = a_n\{X_n\} \tag{A4b}$$

where, by definition,

$$x_n \equiv \{X_n\}^T\{X_I\} \tag{A5a}$$

$$a_n \equiv \{X_n\}^T\{A_I\} \tag{A5b}$$

Substituting Eqs. (A4) into Eq. (A3) gives

$$x_n\{X_n\} = a_n[K]^{-1}[M]\{X_n\} \tag{A6}$$

Substituting the identity from Eq. (A1a) into Eq. (A6) gives

$$x_n\{X_n\} = \left(a_n/\omega_n^2\right)\{X_n\}$$

which, for any nonzero mode $\{X_n\}$, reduces to the following identity:

$$x_n = a_n/\omega_n^2 \tag{A7}$$

The general solution for the deformation due to inertial loading is found by substituting Eq. (A7) into Eq. (A4a):

$$\{X_I\} = \left(a_n/\omega_n^2\right)\{X_n\} \tag{A8}$$

The rms magnitude of deformation is given by the norm (i.e., the square root of the inner product) of the deformation vector. When it is recalled that the basis of normal modes $\{X_n\}$ satisfy Eq. (A1b), the rms magnitude of deformation reduces to

$$x_{\text{rms}} \equiv \|X_I\| = \sqrt{\{X_I\}^T\{X_I\}} = \sqrt{\sum_n \left(\frac{a_n}{\omega_n^2}\right)^2} \tag{A9}$$

Similarly, from Eq. (A4b) the rms magnitude of the inertial acceleration a_{rms} reduces to

$$a_{\text{rms}} = \sqrt{\sum_n a_n^2} \tag{A10}$$

Note that Eqs. (A9) and (A10) are exact if all modes, that is, all values of n are included in the summation.

Equation (A9) can be modified by normalizing the vibration frequencies ω_n by the lowest, that is, fundamental, vibration frequency ω_0. The result is

$$x_{\text{rms}} = \frac{1}{\omega_0^2}\sqrt{\sum_n a_n^2\left(\frac{\omega_0}{\omega_n}\right)^4} \tag{A11}$$

Because $(\omega_0/\omega_n) \leq 1$, Eqs. (A10) and (A11) lead to the following upper bound for the deformation magnitude:

$$x_{\text{rms}} \leq \frac{a_{\text{rms}}}{\omega_0^2} \leq \frac{a_{\text{rms}}}{4\pi^2 f_0^2} \tag{A12}$$

where f_0 is the vibration frequency (in hertz) of the fundamental mode.

In many cases, the system response is dominated by a mode other than the fundamental mode. In these cases, a better estimate for the magnitude of the deformation can be derived by substituting the frequency of the dominant mode (rather than f_0) into Eq. (A12).

Appendix B: Inertial Disturbance Loads

The quasi-static disturbance loads that can affect the dimensional precision of a large space telescope include gravity gradient loads, slew loads, and solar-pressure loads. Appendix B will present bounding linear analyses for the inertial accelerations and deformations caused by each of these disturbances. Numerical results will be presented for two extreme cases: a 25-m gossamer telescope mirror ($\rho_{\text{areal}} = 1$ kg/m^2 $f_0 = 1$ Hz) and the 2.4-m HST mirror ($\rho_{\text{areal}} \approx 200$ kg/m^2 and $f_0 \approx 100$ Hz).

Gravity Gradient Loads

The strength of a gravitational field varies with position in the field. Therefore, any finite sized body in a gravitational field experiences a slightly varying gravitational acceleration across its span. For the body to move as a rigid body through the gravitational field, internal forces develop to compensate for the slight variations in gravitational forces. For a large orbiting telescope, these forces can be large enough to distort the optic appreciably.

A point mass at a distance R from an attracting body experiences an inertial gravitational acceleration of magnitude:

$$|A_i|_{\text{grav}} = \mu/R^2 \tag{B1}$$

where μ is the product of the mass of the attracting body and the universal gravitational constant.[10] Similarly, an orbiting telescope with a mirror of diameter d, aligned along the radial direction to the attracting body, experiences a maximum variation in gravitational acceleration across the mirror, that is, gravity gradient, given by

$$\Delta|A_i|_{\text{grav}} = (\mu/R^2)[1/(1 - d/2R)^2 - 1/(1 + d/2R)^2]$$
$$\cong 2\mu d/R^3 \tag{B2}$$

The period of a circular orbit T_{orb} is related to the radius of the orbit R and μ by

$$(2\pi/T_{\text{orb}})^2 = \mu/R^3 \tag{B3}$$

Hence, from Eqs. (B2) and (B3), the maximum variation in gravitational acceleration across a telescope mirror of diameter d, in a circular orbit of period T_{orb}, is simply

$$\Delta|A_i|_{\text{grav}} \cong 2d(2\pi/T_{\text{orb}})^2 \tag{B4}$$

For a 25-m gossamer telescope mirror orbiting in low Earth orbit ($T_{\text{orb}} \approx 5400$ s), the variation in gravitational acceleration is approximately 6.8×10^{-5} m/s^2 (7 μg). Low Earth orbit represents a worst-case orbit for gravity gradient loading, and other orbits can be expected to result in much lower inertial loading. Because of its smaller diameter, the 2.4-m HST mirror only experiences about 0.7 μg of gravity gradient loading in low Earth orbit.

The magnitude of elastic deformation in the mirror due to gravity gradient inertial loading is bounded by the result given in Appendix A, Eq. (A12). If the rms magnitude of the inertial acceleration is approximately equal to one-half of the maximum variation in gravitational acceleration, that is, $\Delta|A_I|/2$, Eqs. (A12) and (B2) give the following bound on the rms magnitude of elastic deformation:

$$(x_{\text{rms}})_{\text{grav}} \le \frac{(a_{\text{rms}})_{\text{grav}}}{4\pi^2 f_0^2} \le \frac{\Delta|A_i|_{\text{grav}}}{8\pi^2 f_0^2} \le \frac{d}{(f_0 T_{\text{orb}})^2} \tag{B5}$$

For the case of a 25-m gossamer mirror with a first frequency of 1 Hz, the maximum deformation due to gravity gradient loading is approximately 0.9 μm rms. As a contrast, the 2.4-m HST mirror with a first frequency of about 100 Hz experiences a maximum deformation of only about eight pm. Clearly, gravity gradient induced deformations are well below the threshold of interest for HST, but may be of concern for future gossamer telescope mirrors.

Slewing Loads

An orbiting telescope undergoing a constant-rate slew with period T_{slew} (relative to an inertial reference frame) experiences a variation in centrifugal acceleration across the primary mirror of approximately

$$\Delta|A_i|_{\text{slew}} \cong d(2\pi/T_{\text{slew}})^2 \tag{B6}$$

Just as for the case of gravity gradient loading, the variation in centrifugal acceleration during slewing causes an inertial loading of the telescope mirror, which results in internal loads and elastic deformations of the mirror. The magnitude of elastic deformation in the mirror due to this inertial loading is bounded by the result given in Eq. (A12). If the rms magnitude of the inertial acceleration is approximately equal to one-half of the maximum variation in gravitational acceleration, that is, $\Delta|A_I|/2$, the following equation bounds the rms magnitude of elastic deformation due to slewing:

$$(x_{\text{rms}})_{\text{slew}} \le d \Big/ 2(f_0 T_{\text{slew}})^2 \tag{B7}$$

Equations (B6) and (B7) are very similar to Eqs. (B4) and (B5), except for a factor of two, and the period of interest is the slewing period instead of the orbital period. Typically, slew rates will be much faster than orbital precession rates. Hence, inertial loads due to slewing will be much greater than loads due to gravity gradient. However, it is not typically critical for the mirror to maintain figure during slewing, whereas it is critical for it to maintain figure under the influence of gravity gradient loading.

For the case of a 25-m gossamer mirror with $f_0 = 1$ Hz and a slew rate of 1 deg/s ($T_{\text{slew}} = 360$ s) the maximum deformation during slewing will be approximately 96 μm rms. As a contrast, the 2.4-m HST mirror with $f_0 = 100$ Hz experiences a maximum deformation of less than 1 nm during a slew of 1 deg/s. Once again, slew-induced deformations are well below the threshold of interest for HST, but may be of concern for future gossamer telescope mirrors.

Solar Pressure Loads

Of course, the mirrors on infrared space telescopes, for example, NGST, will be shielded from all solar illumination to maintain cryogenic operating temperatures. However, it is conceivable that the backside of some future (noninfrared) gossamer telescope mirrors might see direct solar illumination, and for very low areal density mirrors, the pressure due to direct solar illumination might cause significant deformations.

Solar radiation exerts a pressure according to the following relationship[11]:

$$p_{\text{solar}} = 4.5 \times 10^{-6}\left(k \Big/ R_{\text{solar}}^2\right)(N/m^2) \tag{B8}$$

where k is an accommodation coefficient characterizing the interaction of the incident photon flux with the spacecraft surface, and R_{solar} is the distance from the spacecraft to the sun [in astronomical units (AU)]. The value of k ranges between $1 \le k \le 2$, where $k = 1$ implies a total absorption of the photon flux and $k = 2$ implies a perfect reflection in the direction toward the sun.

An upper bound for the rms magnitude of inertial acceleration due to solar pressure can be found by setting $k = 2$ in Eq. (B8) and dividing by the average areal density of the mirror ρ_{areal}:

$$(a_{\text{rms}})_{\text{solar}} \le \frac{9.0 \times 10^{-6}}{\rho_{\text{areal}} R_{\text{solar}}^2} \frac{m}{s^2} \tag{B9}$$

A body with uniformly distributed mass (i.e., constant value of ρ_{areal}) and a uniform surface specularity (constant value of k) would experience a uniform acceleration in response to the solar pressure. Hence, such a body would not experience any elastic deformation. However, a body with nonuniform mass distribution or surface specularity would be expected to deform elastically as well as accelerate (inertially) in reaction to the solar pressure. An upper bound for the rms magnitude of elastic deformation due to solar pressure is defined by

$$(x_{\text{rms}})_{\text{solar}} \le \frac{(a_{\text{rms}})_{\text{solar}}}{4\pi^2 f_0^2} \le \frac{2.28 \times 10^{-7}}{f_0^2 \rho_{\text{areal}} R_{\text{solar}}^2} m \tag{B10}$$

where f_0 is in hertz, ρ_{areal} is in kilograms per square meter, and R_{solar} is in AU.

For example, the 25-m gossamer telescope mirror with $\rho_{\text{areal}} = 1$ kg/m^2 and $f_0 = 1$ orbiting near the Earth, that is, $R_{\text{solar}} = 1$ AU, could be expected to see accelerations due to solar pressure no greater than 9×10^{-6} m/s^2 (0.92 μg). Furthermore, this loading can be expected to induce deformations in the mirror no greater than 0.23 μm rms. By contrast, if the HST primary mirror were to be illuminated by direct sunlight in its low-Earth orbit, it would be expected to exhibit deformations no greater than 0.1 pm. Once again, deformations from solar pressure loading are of no consequence to the HST but could be significant for future gossamer mirrors.

The preceding analyses have shown that quasi-static inertial loads can easily be on the order of 0.1–10 μg and (for a gossamer mirror) induced deformations can easily be on the order of 1–100 μm rms. Although it is possible to reduce these inertial loads through prudent selection of orbit and operational considerations, for example, slew-rate limitations, it is also prudent to assume some lower limit of uncertainty for inertial loading that must be tolerated by the mirror. For example, it might be reasonable to assume that any mirror system must tolerate at least 1 μg of uncertainty in inertial loading during operations. This assumption leads to the need for robustness in the design of the mirror structure and active control systems.

References

[1]Dressler, A., (ed.), "Exploration and the Search for Origins: A Vision for Ultraviolet–Optical–Infrared Astronomy," *Report of the HST and Beyond Committee*, Association of Univs. for Research in Astronomy, Washington, DC, 1996, pp. 1–7.

[2]Bely, P. Y., Perrygo, C., and Burg, R., "NGST 'Yardstick' Mission," NGST Monograph 1, Next Generation Space Telescope Project Office, NASA Goddard Space Flight Center, July 1999, URL: http://ngst.gsfc.nasa.gov/cgi-bin/doc?Id=597 [cited 15 January 2001].

[3]Lake, M. S., Hachkowski, M. R., "Design of Mechanisms for Deployable Optical Instruments: Guidelines for Reducing Hysteresis," NASA TM 2000-210089, March 2000.

[4]Wu, K. C., and Lake, M. S., "Natural Frequency of Uniform and Optimized Tetrahedral Truss Platforms," NASA TP-3461, Nov. 1994.

[5]Blevins, R. D., *Formulas for Natural Frequency and Mode Shape*, Krieger, Malabar, FL., 1995, pp. 224–229.

[6]Timoshenko, S. P., and Gere, J. M., *Theory of Elastic Stability*, 2nd ed., McGraw–Hill, New York, 1961, pp. 317, 318.

[7]Hedgepeth, J. M., "Critical Requirements for the Design of Large Space Structures," NASA CR-3484, Nov. 1981.

[8]Creedon, J. F., "Discrete Control of Linear Distributed Systems with Application to the Deformable Primary Mirror of a Large Orbiting Telescope," Ph.D. Dissertation, Dept. of Electrical Engineering, Univ. of Rhode Island, Kingston, RI, 1970.

[9]Dettman, J. W., *Mathematical Methods in Physics and Engineering*, 2nd ed., Dover, New York, 1969, pp. 123, 124.

[10]Danby, J. M. A., *Fundamentals of Celestial Mechanics*, 2nd ed., Willman–Bell, Richmond, VA, 1988, pp. 63–65.

[11]Griffin, M. D., and French, J. R., *Space Vehicle Design*, 1st ed., AIAA, Washington, DC, 1991, pp. 128–130.

C. Jenkins
Guest Editor